Thermochemistry of iron manganese oxide spinels

Sophie Guillemet-Fritsch[a], Alexandra Navrotsky[b],*, Philippe Tailhades[a],
Hervé Coradin[a], Miaojun Wang[b]

[a]*Centre InterUniversitaire de Recherche et d'Ingénierie des Matériaux (CIRIMAT/LCMIE), Université Paul Sabatier, Bâtiment 2R1,
118, route de Narbonne, 31062 Toulouse, Cedex 04, France*
[b]*Thermochemistry Facility and NEAT ORU, The University of California at Davis, One Shields Avenue, Davis, CA 95616-877, USA*

Abstract

Oxide melt solution calorimetry has been performed on iron manganese oxide spinels prepared at high temperature. The enthalpy of formation of $(Mn_xFe_{1-x})_3O_4$ at 298 K from the oxides, tetragonal Mn_3O_4 (hausmannite) and cubic Fe_3O_4 (magnetite), is negative from $x = 0$ to $x = 0.67$ and becomes slightly positive for $0.67 < x < 1.0$. Relative to cubic Mn_3O_4 (stable at high temperature) and cubic Fe_3O_4 (magnetite), the enthalpy of formation is negative for all compositions. The enthalpy of formation is most negative near $x = 0.2$. There is no significant difference in the trend of enthalpy of formation versus composition for cubic ($x < 0.6$) and tetragonal ($x > 0.6$) spinels of intermediate compositions. The enthalpies of formation are discussed in terms of three factors: oxidation–reduction relative to the end-members, cation distribution, and tetragonality. A combination of measured enthalpies and Gibbs free energies of formation in the literature provides entropies of mixing. ΔS_{mix}, consistent with a cation distribution in which all trivalent manganese is octahedral and all other ions are randomly distributed for $x > 0.5$, but the entropy of mixing appears to be smaller than these predicted values for $x < 0.4$.

1. Introduction

Manganese iron oxide spinels $((Mn_xFe_{1-x})_3O_4)$ have been the subject of extensive research because of their potential applications to magnetic recording media and electronic devices. The phase diagram of Mn_3O_4–Fe_3O_4 is well known at high temperature [1–7]. The spinel $(Mn_xFe_{1-x})_3O_4$ is generally obtained in air at temperatures above 1223 K. The structure can be cubic or tetragonal. This structural transition occurs at $x = 0.6$ for samples quenched to room temperature, as the concentration of Mn^{3+} cations becomes sufficiently high to lead to cooperative Jahn–Teller distortion. At room temperature the degree of distortion, measured by the crystallographic c/a ratio, decreases from 1.16 at

$x = 1$ to 1.00 at $x = 0.6$ and below. This system also shows a magnetic transition from ferrimagnetic to paramagnetic at $x = 0.8$ at room temperature. Structural and magnetic studies suggest that the physical properties of these spinels vary with conditions of preparation, as do the cation distributions and oxygen contents.

For $x = 1$, the tetragonal-to-cubic transition occurs at 1445 K with $\Delta H = 20.8 \, kJ \, mol^{-1}$ and $\Delta S = 14.4 \, J \, K^{-1} \, mol^{-1}$ [8]. For $0.6 < x < 1$, the transition presumably occurs at intermediate temperatures, but its thermodynamic properties have not been determined.

The coexistence of both cubic and tetragonal phases over a small composition range has been reported [9,10]. Mason [1] described vredenburgite (name no longer in use), a mineral formed by an intergrowth of the mineral jacobsite ($MnFe_2O_4$) and hausmannite (Mn_3O_4). Even if the phases are prepared at low temperature by

coprecipitation techniques, a lack of miscibility of the system Mn_3O_4–Fe_3O_4 is sometimes seen [11].

Some thermodynamic data (from which Gibbs free energies of formation and activity–composition relations can be estimated) have been reported for the system Mn_3O_4–Fe_3O_4 [12–20], but they are incomplete and of varying accuracy. The enthalpy of formation of $MnFe_2O_4$ ($x = 0.33$) has been measured by solution calorimetry in hot phosphoric acid [21]. To our knowledge, no other direct calorimetric measurements of enthalpy of formation have been made in this system. However, the energetics of some binary manganese oxides [22,23] and iron oxides [24,25] has been studied by high-temperature oxide melt calorimetry. The present study extends such measurements to well-characterized mixed iron manganese oxide spinels.

2. Experimental procedures

2.1. Sample preparation

Pure hematite (α-Fe_2O_3) and bixbyite (α-Mn_2O_3) from Aldrich Chemical Co. (99.999%) have been dried at 373 K for 4 h prior to calorimetry. The spinel phases $(Mn_xFe_{1-x})_3O_4$ have been prepared by the thermal decomposition of $(Mn_xFe_{1-x})C_2O_4 \cdot 2H_2O$ precursors prepared from the coprecipitation of transition metal chlorides ($FeCl_2 \cdot 4H_2O$, and $MnCl_2 \cdot 4H_2O$) and oxalic acid ($H_2C_2O_4 \cdot 2H_2O$). These oxalates were treated at 1673 K for $x < 0.33$ and at 1373 K for $x > 0.33$ in air, according to the phase diagram [5]. The cycle consisted of a temperature rise at $200\,K\,h^{-1}$, a dwell of 2 h and a quench in air. The powders were ground, sieved to $80\,\mu m$ and stored in a desiccator prior to calorimetry.

2.2. Characterization

A Siefert diffractometer, equipped with a SiLi detector and using CuKα radiation ($\lambda = 0.15418\,nm$) was used for XRD analysis. The chemical composition was determined by inductively coupled plasma (ICP) spectroscopy (ICP Maxim, Thermo-opteck). Thermogravimetric analysis (TGA) was performed using a Setaram TAG 24 apparatus and DTA by a Setaram TAG92. Additional TGA was done using a Netzsch 409 apparatus.

2.3. High-temperature oxide melt solution calorimetry

High-temperature drop solution calorimetry was performed using a Tian Calvet twin-type calorimeter described by Navrotsky [26,27]. The solvent was $3Na_2O \cdot 4MoO_3$ at 976 K. The calibration factor was obtained by dropping, into an empty Pt crucible in the calorimeter, pellets of known mass (and enthalpy) of pure α-Al_2O_3 (99.99%, Aldrich, stabilized in the corundum phase by heating at 1773 K for 24 h).

The samples were pressed into pellets of approximately 5 mg, weighed on a semi-micro balance, and dropped from room temperature into a platinum crucible containing approximately 15 g of solvent equilibrated overnight in the calorimeter. Pure oxygen was used for flushing the calorimetric system (at $76\,mL\,min^{-1}$) and for bubbling through the solvent (at $4.75\,mL\,min^{-1}$). The oxygen bubbling stirs the melt, enhances the dissolution rate of the pellets, and defines the final oxidation state of the dissolved species in the melt. Rapid oxidation of the spinels to Mn_2O_3 and Fe_2O_3 in air at 976 K has been confirmed by TGA and XRD analysis. When samples are dropped into the melt, they undergo oxidation/reduction and dissolution sequentially and/or simultaneously.

The final oxidation state of Mn and Fe in the solvent must be reproducible and the same regardless of the initial oxidation state of the samples. The oxidation state of iron dissolved in molten sodium molybdate under oxygen or air is ferric, regardless of the initial oxidation state [24,25,28,29].

The oxidation state of manganese in sodium molybdate at 974–977 K was determined by in situ weight change experiments conducted on a Netzsch STA 409 TGA/DTA analyzer. The experiments were run in TG mode only (no thermal analysis) with a sample carrier and alumina crucible that can accommodate a relatively large sample volume (~6 mL). The sodium molybdate solvent (~4.8 g) was heated in a small platinum crucible (which fits into the alumina TGA crucible) and brought to constant weight before the TG experiment. A baseline was obtained with the crucible and solvent only. The manganese oxide powder was added and the TG runs were heated in oxygen at $10\,K\,min^{-1}$ and held at 974–977 K for 1.5 h to attain equilibrium. The accuracy of the TG experiments was checked by dissolving Co_3O_4 in sodium molybdate at 974 K under argon (with known weight loss of 6.64% to form dissolved CoO). The observed weight loss was 6.50% and 6.72% (two runs). For manganese oxides, Table 1 shows that there is the same mixture of oxidation states in the melt ($11.3 \pm 0.3\%$ trivalent, $88.7 \pm 0.3\%$ divalent) regardless of the starting oxidation state. Note that the data for weight changes on dissolution of MnO, which give 16.6% Mn^{3+}, are less accurate because of the very small weight changes involved, and we interpret them as being consistent with the experiments on other manganese oxides. Thus the final state of manganese in the solvent, though a mixture of oxidation states, is reproducible and constant and is thus suitable for calorimetry.

Additional experiments have been performed in a furnace to check the rate of dissolution of the samples in the molten sodium molybdate at 976 K. After 30 min without agitation, no trace of powder was visible.

Table 1
Final state of manganese in $3Na_2O \cdot 4MoO_3$ melt at 974–977 K in oxygen as measured by in situ thermogravimetry

Sample	Sample mass (mg)	Weight change (mg)	Weight change (%)	Average (%)	Mn^{2+} (mol %)	Mn^{3+} (mol %)
MnO_2	36.33	−6.26	−17.23	−17.39	99.0	11.0
	42.87	−7.52	−17.55			
Mn_2O_3	52.40	−4.85	−9.26	−8.99	88.7	11.3
	49.60	−4.48	−9.04			
	53.48	−4.64	−8.68			
Mn_3O_4	51.23	−2.94	−5.73	−5.78	88.4	11.6
	52.05	−3.03	−5.83			
MnO	39.90	+0.89	+2.23	+1.87	83.4[a]	16.6
	40.16	+0.61	+1.51			

[a]Value considered less accurate because of small weight change. However, the observed sign of change (weight gain) confirms reversibility and that the oxidation state in the melt is a mixture of Mn^{2+} and Mn^{3+}.

The shape of the calorimetric curve, which returned to baseline in less than an hour, and reproducible enthalpies also are consistent with rapid dissolution. Calorimetric experiments were limited to 6 or fewer consecutive drops of 15 mg pellets per 15 g batch of solvent, both to ensure the Henry's Law regime (constant enthalpy of solution) and to avoid slower dissolution rates at higher concentrations. A minimum of eight experiments for each composition produced a maximum standard deviation of 1%. The samples prepared at high temperature present low specific surface areas (BET surface area $\sim 1 \, m^2 \, g^{-1}$) and no water loss was seen by TGA. Thus no corrections to the calorimetric data for surface area or adsorbed water were necessary.

Fig. 1. Variation of the unit cell parameters (a and c) of the $(Mn_xFe_{1-x})_3O_4$ system as a function of the Mn content, x.

3. Results and discussion

3.1. Unit cell parameters

X-ray diffraction shows a cubic spinel structure ($Fd3m$) for $0 < x < 0.6$ and a tetragonal one ($I41/amd$) for $x > 0.6$. The cell parameters, calculated by Rietveld analysis [30], are presented in Fig. 1. They are in good agreement with previous data for stoichiometric ($Mn_x Fe_{1-x})_3O_4$ spinels [31–34]. This agreement and the high-temperature preparation conditions lead to the conclusion that the spinels used for calorimetry are stoichiometric in oxygen, with $(Mn + Fe)/O = 0.75$.

3.2. Measured enthalpies

Table 2 gives the measured enthalpies of drop solution. Using the data for the end-members, Fe_3O_4 and Mn_3O_4, we checked for consistency in enthalpies of oxidation/reduction, according to thermodynamic cycles I and II in Table 3. The enthalpy of drop solution of Mn_3O_4 and Fe_3O_4, 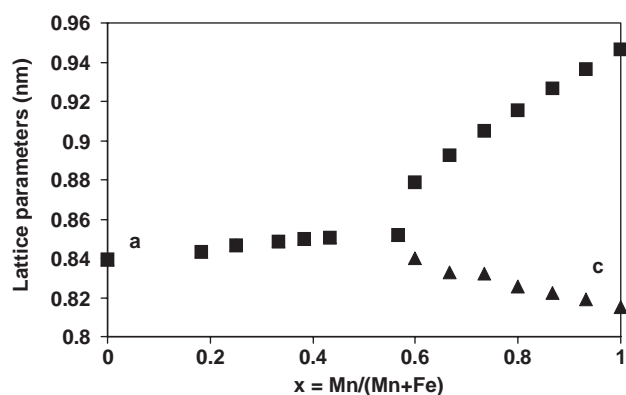was recalculated starting from the values obtained for Mn_2O_3 and Fe_2O_3, which were corrected for the enthalpy of oxidation of Mn_3O_4 into Mn_2O_3 and Fe_3O_4 into Fe_2O_3 [8,35,36]. The calculated values of $\Delta H_{dropsol}$, $168.1 \, kJ \, mol^{-1}$ for Mn_3O_4 and $15.4 \, kJ \, mol^{-1}$ for Fe_3O_4 (with propagated errors of about $\pm 4 \, kJ \, mol^{-1}$) agree with the measured data, 170.6 ± 1.0 and $17.1 \pm 2.9 \, kJ \, mol^{-1}$ (Table 2). This is further evidence for reproducible final oxidation states of Fe and Mn in the molten solvent.

Thermodynamic cycle (III) (Table 3) was used to calculate the enthalpy of formation of $(Mn_xFe_{1-x})_3O_4$ from the oxides t-Mn_3O_4 and c-Fe_3O_4, $\Delta H_{f,(t,c)}$, where t is tetragonal, c is cubic (see Fig. 2). This reaction is

$$x Mn_3O_4(t) + (1-x)Fe_3O_4(c)$$
$$= (Mn_xFe_{1-x})_3O_4(t \text{ or } c), \quad \Delta H_{f,(t,c)}. \quad (1)$$
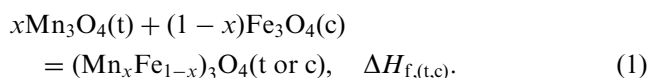
The data can be fitted by a cubic polynomial, constrained to be zero at $x = 0$ and 1 (see Fig. 2a)

$$\Delta H_{f(t,c)}(kJ \, mol^{-1}) = -418.51 \, x^3 + 703.49 \, x^2 - 284.98 \, x$$
$$(0 \leqslant x \leqslant 1) \quad (2)$$

Table 2

Measured enthalpy of drop solution in $3Na_2O \cdot 4MoO_3$ at 976 K and calculated enthalpy of formation at 298 K of iron manganese oxide spinels from tetragonal Mn_3O_4 and cubic Fe_3O_4

Phase (x)	Structure (mineral name) [c/a ratio]	Enthalpy of drop solution, $\Delta H_{dropsol}$ (kJ mol^{-1})	Enthalpy of formation at 298 K from tetragonal Mn_3O_4 and cubic Fe_3O_4, $\Delta H_{f(t\text{-}c)}$ (kJ mol^{-1})
α-Mn_2O_3	Cubic (bixbyite)	151.7 ± 1.0[a]	
α-Fe_2O_3	Rhombohedral (hematite)	96.3 ± 0.7	
Fe_3O_4 (0.00)	Cubic spinel (magnetite)	17.1 ± 2.9[b]	0
$Mn_{0.55}Fe_{2.45}O_4$ (0.18)	Cubic spinel	89.3 ± 1.2	-44.1 ± 2.7[c]
$Mn_{0.72}Fe_{2.28}O_4$ (0.24)	Cubic spinel	89.8 ± 1.0	-35.9 ± 2.4
$Mn_{1.03}Fe_{1.97}O_4$ (0.34)	Cubic spinel	99.3 ± 1.4	-29.5 ± 2.4
$Mn_{1.21}Fe_{1.79}O_4$ (0.40)	Cubic spinel	102.5 ± 1.8	-23.5 ± 2.5
$Mn_{1.30}Fe_{1.70}O_4$ (0.43)	Cubic spinel	106.4 ± 1.8	-22.8 ± 2.5
$Mn_{1.74}Fe_{1.26}O_4$ (0.58)	Cubic spinel	115.6 ± 1.5	-9.5 ± 2.0
$Mn_{1.84}Fe_{1.16}O_4$ (0.61)	Tetragonal spinel [1.05]	109.5 ± 1.9	1.7 ± 2.3
$Mn_{2.05}Fe_{0.95}O_4$ (0.68)	Tetragonal spinel [1.07]	118.5 ± 1.3	3.5 ± 1.7
$Mn_{2.21}Fe_{0.79}O_4$ (0.74)	Tetragonal spinel [1.08]	130.7 ± 1.8	-0.5 ± 2.1
$Mn_{2.38}Fe_{0.62}O_4$ (0.79)	Tetragonal spinel [1.10]	144.1 ± 2.5	-5.2 ± 2.7
$Mn_{2.46}Fe_{0.54}O_4$ (0.82)	Tetragonal spinel [1.11]	135.7 ± 1.4	7.3 ± 1.7
$Mn_{2.60}Fe_{0.40}O_4$ (0.87)	Tetragonal spinel [1.12]	138.2 ± 1.6	11.9 ± 1.9
$Mn_{2.80}Fe_{0.20}O_4$ (0.93)	Tetragonal spinel [1.14]	156.4 ± 0.7	4.0 ± 1.2
Mn_3O_4 (1.00)	Tetragonal spinel (Hausmannite) [1.16]	170.6 ± 1.0[b]	0

[a] Uncertainty is two deviations of the mean.
[b] Data are from Laberty and Navrotsky [24].
[c] Propagated error.

A cubic polynomial is necessary to reflect the minimum in enthalpy near $x = 0.2$; a quadratic would force a minimum at $x = 0.5$. Although the cubic polynomial does not fit $\Delta H_{f,(t,c)}$ very well, we doubt that any higher polynomial representation is warranted when one considers the scatter in measured data. Furthermore, because of the changes in redox state, cation distribution, and symmetry, this system cannot be described simply as a subregular solution (as the cubic polynomial might otherwise imply), as discussed below.

The enthalpy of formation of $(Mn_xFe_{1-x})_3O_4$ from cubic magnetite and tetragonal hausmannite is negative from $x = 0$ to 0.67, and becomes slightly positive for $0.67 < x < 1.0$ (see Fig. 2a). This change occurs near the symmetry change of the spinel phase from tetragonal to cubic.

The enthalpy of formation appears to have a minimum near $x = 0.2$. Spinels with $x < 0.18$ could not be prepared by the techniques used here so the very iron-rich part of the curve is not well constrained, though, by definition, $\Delta H_{f,(t,c)}$ has to be zero at $x = 0$. Navrotsky [17] argued that the oxidation–reduction enthalpy for the reaction

$$Fe^{2+} + Mn^{3+} = Fe^{3+} + Mn^{2+} \qquad (3)$$
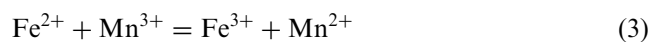
dominates the energetics of this solid solution series, with Fe^{2+} present only at $x < 0.33$, and, using oxidation–reduction enthalpies for binary oxides, calculated $\Delta H_{f,(t,c)}$ for the system, with a minimum at $MnFe_2O_4$

($x = 0.33$) of -17.6 kJ mol^{-1}. The calorimetric data show a deeper minimum, -44.1 kJ mol^{-1} at $x = 0.18$ and -29.5 kJ mol^{-1} at $x = 0.33$ (measured) or -31.3 kJ mol^{-1} at $x = 0.18$ and -32.4 kJ mol^{-1} at $x = 0.33$ (calculated using Eq. (2)). Thus though the simple model is a reasonable first approximation, the redox reactions and other factors may play an even more stabilizing role in the spinels than in the binary oxides.
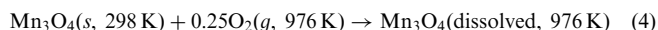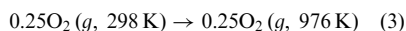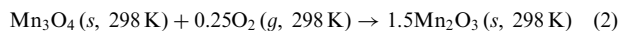
Reznitskii et al. [21] reported the enthalpy of formation of $MnFe_2O_4$ based on solution calorimetry of MnO, Fe_2O_3, and $MnFe_2O_4$ in phosphoric acid at 140 °C. Recalculated to reaction (1), their data give $\Delta H_{f,(t,c)} = -17$ kJ mol^{-1}. The reference does not give much detail about procedures, sample characterization, and oxidation states upon dissolution, so the accuracy of this determination is difficult to assess.

$\Delta H_{f,(t,c)}$ can also be approximated by two straight line segments (one defined by $x = 0$ and 0.18 and the other by $0.18 < x < 1$, excluding the point for tetragonal hausmannite, as shown in Fig. 2. The data for $0.18 < x < 1$ include points for both cubic ($x < 0.6$) and tetragonal ($x > 0.6$) phases. Though the points for $x > 0.6$ scatter more than those for cubic phases, they do not define a noticeably different trend. The equation of this line is

$$\Delta H_{f,(t,c)} \text{ (kJ mol}^{-1}) = 69.86x - 51.87$$

$$(0.18 \leqslant x \leqslant 0.93). \qquad (4)$$

Table 3
Thermodynamic cycles used in calculations

Cycle I: consistency check of heats of drop solution of Mn_2O_3 and Mn_3O_4

$$1.5Mn_2O_3(s,\ 298\,K) \rightarrow 1.5Mn_2O_3(\text{dissolved},\ 976\,K) \quad (1)$$

$$Mn_3O_4\ (s,\ 298\,K) + 0.25O_2\ (g,\ 298\,K) \rightarrow 1.5Mn_2O_3\ (s,\ 298\,K) \quad (2)$$

$$0.25O_2\ (g,\ 298\,K) \rightarrow 0.25O_2\ (g,\ 976\,K) \quad (3)$$

$$Mn_3O_4(s,\ 298\,K) + 0.25O_2(g,\ 976\,K) \rightarrow Mn_3O_4(\text{dissolved},\ 976\,K) \quad (4)$$

Dissolved = final reproducible dissolved state in sodium molybdate at 976 K as discussed in text
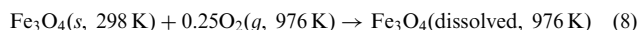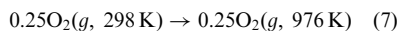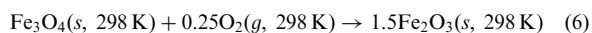$\Delta H_1 = 1.5$ (enthalpy of drop solution of Mn_2O_3) = 227.6 kJ mol^{-1}
$\Delta H_2 =$ enthalpy of oxidation of Mn_3O_4 to $Mn_2O_3 = 1.5\Delta H_{f,el}(Mn_2O_3) - \Delta H_{f,el}\ (Mn_3O_4) = -54.0$ kJ mol^{-1} [36]
($\Delta H_{f,el} =$ enthalpy of formation from the elements) [36]
$\Delta H_3 = 0.25\ (H_{976} - H_{298})O_2) = 5.5$ kJ mol^{-1} [36]
Then $\Delta H_4 = \Delta H_1 + \Delta H_2 - \Delta H_3 = 227.6 - 54.0 - 5.5 = 168.1$ kJ mol^{-1}

Cycle II: consistency check of heats of drop solution of Fe_2O_3 and Fe_3O_4

$$1.5Fe_2O_3(s,\ 298\,K) \rightarrow 1.5Fe_2O_3(\text{dissolved},\ 976\,K) \quad (5)$$

$$Fe_3O_4(s,\ 298\,K) + 0.25O_2(g,\ 298\,K) \rightarrow 1.5Fe_2O_3(s,\ 298\,K) \quad (6)$$

$$0.25O_2(g,\ 298\,K) \rightarrow 0.25O_2(g,\ 976\,K) \quad (7)$$

$$Fe_3O_4(s,\ 298\,K) + 0.25O_2(g,\ 976\,K) \rightarrow Fe_3O_4(\text{dissolved},\ 976\,K) \quad (8)$$

Dissolved = final reproducible dissolved state in sodium molybdate at 976 K as discussed in text
ΔH_5: 1.5 (enthalpy of drop solution of Fe_2O_3) = 144.5 kJ mol^{-1}
$\Delta H_6 =$ enthalpy of oxidation of Fe_3O_4 to $Fe_2O_3 = 1.5\ \Delta H_{f,el}\ (Fe_2O_3) - \Delta H_{f,el}\ (Fe_3O_4) = -123.6$ kJ mol^{-1} [36]
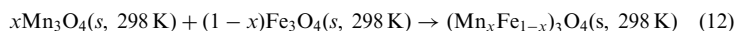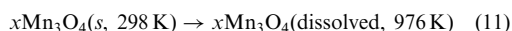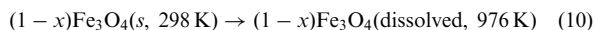($\Delta H_{f,el} =$ enthalpy of formation from the elements) [36]
$\Delta H_7 = 0.25\ (H_{976} - H_{298})O_2) = 5.5$ kJ mol^{-1} [36]
Then $\Delta H_8 = \Delta H_5 + \Delta H_6 - \Delta H_7 = 144.5 - 123.6 - 5.5 = 15.4$ kJ mol^{-1}
Note, in cycles I and II, the reactions are written as though the dissolved ions are trivalent for simplicity. As long as the oxidation states in the solvent are the same whether starting with Mn_3O_4 or Mn_2O_3, the cycles still are valid, even though, see text, the dissolved manganese is more reduced than Mn^{3+}

Cycle III: enthalpy of formation of $(Mn_xFe_{1-x})_3O_4$ from Mn_3O_4 and Fe_3O_4

$$(Mn_xFe_{1-x})_3O_4(s,\ 298\,K) \rightarrow (Mn_xFe_{1-x})_3O_4(\text{dissolved},\ 976\,K) \quad (9)$$

$$(1-x)Fe_3O_4(s,\ 298\,K) \rightarrow (1-x)Fe_3O_4(\text{dissolved},\ 976\,K) \quad (10)$$

$$xMn_3O_4(s,\ 298\,K) \rightarrow xMn_3O_4(\text{dissolved},\ 976\,K) \quad (11)$$

$$xMn_3O_4(s,\ 298\,K) + (1-x)Fe_3O_4(s,\ 298\,K) \rightarrow (Mn_xFe_{1-x})_3O_4(s,\ 298\,K) \quad (12)$$

ΔH_9: enthalpy of drop solution of 1 mol of $(Mn_xFe_{1-x})_3O_4$ (see Table 1)
ΔH_{10}: enthalpy of drop solution of $Fe_3O_4 = 17.1 \pm 2.9$ kJ mol^{-1}
ΔH_{11}: enthalpy of drop solution of $Mn_3O_4 = 170.6 \pm 1.0$ kJ mol^{-1}.
ΔH_{12}: enthalpy of formation at 298 K of the spinel $(Mn_xFe_{1-x})_3O_4$ from the oxides Fe_3O_4 and $Mn_3O_4 = \Delta H_{12} = -\Delta H_9 + (1-x)\Delta H_{10} + x\Delta H_{11}$
This cycle holds as long as the final state of Mn and Fe in the melt are reproducible and the same throughout all experiments, regardless of what the oxidation states in the melt actually are (see text)
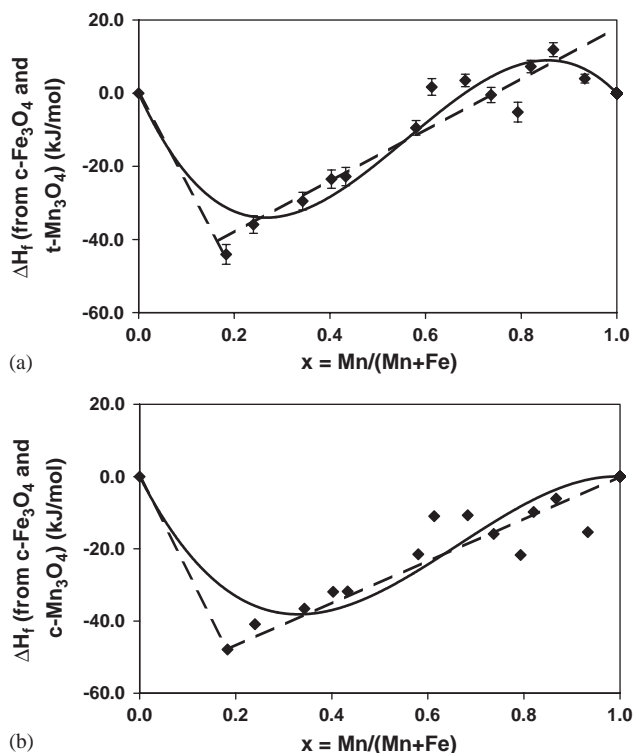
Fig. 2. (a) Enthalpy of formation of $(Mn_xFe_{1-x})_3O_4$ (tetragonal or cubic) from tetragonal Mn_3O_4 (hausmannite) and cubic Fe_3O_4 (magnetite) at 298 K ($\Delta H_{f,(t-c)}$) as a function of Mn content, x. (b) Enthalpy of formation of $(Mn_xFe_{1-x})_3O_4$ (tetragonal or cubic) from cubic Mn_3O_4 and cubic Fe_3O_4 at 298 K ($\Delta H_{f,(c-c)}$) as a function of Mn content, x. The curves are the cubic polynomial fits and the dashed lines the straight line segments as discussed in the text.

The extrapolation of this line to $x = 1$ gives $18.0 \pm 3 \, \mathrm{kJ \, mol^{-1}}$. This is the enthalpy of formation of cubic Mn_3O_4 from tetragonal Mn_3O_4 as defined by $\Delta H_{f(t,c)}$ for $x = 1$. In other words, this is the enthalpy of the tetragonal-to-cubic transformation in Mn_3O_4. The tetragonal-to-cubic transformation is reported to occur at 1445 K with a ΔH of $20.8 \, \mathrm{kJ \, mol^{-1}}$ [8]. These values agree within their estimated errors (about $\pm 5 \, \mathrm{kJ \, mol^{-1}}$ for each). Using $\Delta H = 20.8 \, \mathrm{kJ \, mol^{-1}}$, the enthalpy of formation of the observed spinels from cubic Fe_3O_4 and cubic Mn_3O_4

$$x Mn_3O_4(c) + (1 - x) Fe_3O_4(c)$$
$$= (Mn_xFe_{1-x})_3O_4(\text{t or c}), \quad \Delta H_{f,(c-c)} \quad (5)$$
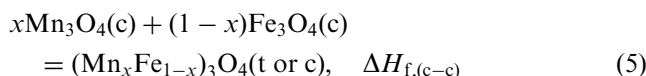
is $\Delta H_{f(c-c)} = \Delta H_{f(t-c)} - 20.8\,x$ (see Fig. 2b). Relative to cubic end-members, all compositions are energetically stable. Once more, the data can be approximated by a cubic polynomial, again constrained to be zero at $x = 0$ and 1

$$\Delta H_{f(c-c)} = -258.57\,x^3 + 514.91\,x^2 - 256.34\,x. \quad (6)$$

Two line segments, one joining the point at $x = 0$ and 0.18 and the other joining the point at $x = 0.18$ and 1 also provide a reasonable representation of the data.

3.3. Tetragonality, cation distribution, magnetism, and energetics

It seems likely that the major contribution to the energetics of reaction (1) arises from the valence distribution, expressed by reaction (3). However, the tetragonal distortion, magnetic transitions, and changes in cation distribution also influence the thermodynamic properties and merit some further discussion. The effect of the tetragonal-to-cubic transition in Mn_3O_4 on the enthalpies of formation of the solid solution at 298 K has been discussed above. Because the tetragonal and cubic spinels of intermediate composition seem to fall on the same trend in enthalpy of formation (see Fig. 2), we conclude that the effect of the tetragonal-to-cubic transition on energetics appears to be small at $0.5 < x < 0.8$, i.e., in the vicinity of the change in symmetry at room temperature. The tetragonality (c/a ratio) also diminishes rapidly with decreasing x (see Fig. 1 and Table 2), so it is reasonable to conclude that $\Delta H_{(t-c)}$ diminishes rapidly from its value of $20.8 \, \mathrm{kJ \, mol^{-1}}$ at $x = 1$ to a very small value near $x = 0.6$, but the functional form of this dependence is not known. However, the enthalpy of formation data between $x = 0.5$ and 1 show considerable scatter and might suggest two maxima separated by a minimum, although such an interpretation is just at the edge of detectability given the experimental errors and is therefore suggestive and not definitive.

The Neel temperature has been determined as a function of Mn content (x) by several authors [37–40]. It decreases linearly with x, and is below room temperature for $x > 0.33$. There are no accurate heat capacity measurements for intermediate compositions, and the effect of this transition on the thermodynamics of mixing cannot be quantified.

The cation distributions in these spinels at both room temperature and at high temperature have been the subject of considerable investigation and a consensus has not yet emerged [41–47]. Whereas it is clear that Mn^{3+} has a strong octahedral preference and occupies exclusively octahedral sites, the site preferences of Mn^{2+}, Fe^{2+}, and Fe^{3+} are not strong [48,49]. Thus their distribution may depend significantly on temperature but because their enthalpies of interchange are small, this changing cation distribution will not strongly affect the heats of formation. Furthermore, because of rapid electron (hole) hopping in magnetite, it is not clear whether Fe^{2+} and Fe^{3+} should be treated as thermodynamically distinct species. Considering the large enthalpy of the oxidation–reduction reaction (Eq. (3)), the uncertainty in the cation distribution of our

quenched samples, and the scatter in the calorimetric data, we have not attempted to derive energetic parameters for cation interchange from our data.

3.4. Entropies of mixing

The studies of Tret'yakov [18] and of Schwerdtfeger and Muan [19] provide activity–composition relations in the Fe_3O_4–Mn_3O_4 system, referring, at high temperature, to cubic spinels. Table 4 lists calculated Gibbs free energies of mixing, i.e., ΔG for Eq. (5), calculated from these data. The entropy of mixing, ΔS for Eq. (5), can be calculated as $\Delta S = (\Delta H - \Delta G)/T$, where ΔH is taken for the cubic spinels (Eq. (6)). The uncertainty in these experimental values of ΔS is hard to estimate, but it is probably between ± 5 and $\pm 8\,J\,mol^{-1}\,K^{-1}$ and arises from uncertainties in the calorimetric data, the approximate fit of Eq. (6) to the calorimetric data, and uncertainties in the activity data.

The experimental entropies of mixing can be compared with the change in configurational entropy calculated assuming Fe_3O_4 is a random spinel, Mn_3O_4 is normal, and intermediate spinels have maximum oxidation of Fe^{2+} to Fe^{3+} and a cation distribution in which Mn^{3+} is octahedral but all other cations are randomly distributed [17]. These theoretical values are also shown in Table 3 and represent the largest (most random) configurational entropy of mixing that can reasonably occur in the system. The experimental

Table 4
Calculation of entropies of mixing in $(Fe_{1-x}Mn_x)_3O_4$ solid solutions

x	ΔG (kJ mol^{-1})	ΔH (kJ mol^{-1})	ΔS (J K^{-1} mol^{-1})	
	(A)	(B)	(C)	(D)
0.1	−14.6 (−15.0)	−20.7	−4.8 (−4.0)	6.7
0.2	−21.7 (−24.1)	−32.7	−8.6 (−6.0)	8.8
0.3	−29.3 (−29.4)	−37.5	−6.3 (−5.7)	7.5
0.4	−37.2	−36.7	0.4	11.1
0.5	−41.0	−31.8	7.2	15.4
0.6	−46.0	−24.3	17.0	17.4
0.7	−46.9	−15.8	24.4	17.6
0.8	−37.7	−7.8	23.5	15.8
0.9	−25.1	−2.1	18.1	11.3

(A) Free energy of mixing (formation from cubic end-member spinels) calculated from activity data. First value is from electrochemical cell study of Tret'yakov [18], taken in middle of temperature range of measurements, 1273 K. Second value (in parentheses) is from gas equilibration studies of Schwerdtfeger and Muan [19] at 1523 K.
(B) Enthalpy of mixing calculated using Eq (6).
(C). Experimentally determined entropy of mixing, $\Delta S = (\Delta H - \Delta G)T$. Estimated uncertainty is ± 5 to $\pm 0.8\,J\,K^{-1}\,mol^{-1}$ (see text).
(D) Configurational entropy of mixing, assuming Mn_3O_4 is a normal spinel, Fe_3O_4 is random, and intermediate spinels have all Mn^{3+} on octahedral sites, with Mn^{2+}, Fe^{2+} and Fe^{3+} randomly distributed.

entropy of mixing at $x < 0.4$ appears to be negative or close to zero. That at $x > 0.4$ scatters around the values predicted by the random model, the experimental values perhaps becoming more positive than those for the random model at $x > 0.6$. There may be several reasons for this behavior. (1) There may be larger systematic errors in the calorimetric and/or the activity data than assumed here. We have no evidence that this would be the case. (2) The entropy model may be inappropriate when both Fe^{2+} and Fe^{3+} are present because of rapid electron exchange, leading to communal electronic entropy rather than a configurational term from positional disorder. The communal entropy arising from electron hopping between Fe^{2+} and Fe^{3+} may be destroyed in the solid solution by the addition of manganese and the oxidation of Fe^{2+} to Fe^{3+}. This would occur at $0 < x < 0.33$ (little or no Fe^{2+} present at $x > 0.33$). The strongly negative enthalpy of mixing and the diminished entropy of mixing in this range may thus reflect electron localization as manganese is substituted for iron. However, quantitative analysis of the communal entropy in either end-member magnetite or in the solid solution is not possible at present. (3) The solid solutions themselves may have more ordered cation distributions. Note that quite extensive order would be required to decrease the entropies substantially. (4) Vibrational entropy terms may be significant. (5) The tetragonal—cubic transition and the Neel transition may not be treated adequately in the calorimetric and/or the activity data, especially for compositions where the solid solutions are tetragonal. We conclude that the random mixing model (with all trivalent manganese octahedral) is a useful starting point for modeling these solid solutions but some additional terms related to the factors above may be needed to refine the model. We stress that a subregular solution model, with Raoultian entropies of mixing ($\Delta S_{mix} = -R[x \ln x + (1-x) \ln (1-x)]$) and ΔH_{mix} given by Eq. (6) is definitely incorrect.

The most negative heats of mixing occur at or below $x = 0.33$. The most negative free energies of mixing occur at $x = 0.6-0.7$. This is clear indication that the $T\Delta S$ term is larger in magnitude than ΔH as manganese content increases. This has been noted previously [17].

4. Conclusions

The system Mn_3O_4–Fe_3O_4 shows strongly negative heats of mixing which are most pronounced at manganese-rich compositions ($Mn/(Mn+Fe) = 0.2-0.3$). The calorimetric data are consistent with a strongly exothermic enthalpy of oxidation–reduction to form Mn^{2+} and Fe^{3+} from Mn^{3+} and Fe^{2+}. The minimum in Gibbs free energy of mixing occurs at $Mn/(Mn+Fe) = 0.6-0.7$, confirming a larger configurational

entropy of mixing at higher manganese contents. The extrapolated enthalpy of the tetragonal to cubic transition in Mn_3O_4 is $18 \pm 5 \, kJ \, mol^{-1}$, confirming an earlier value of $20.8 \, kJ \, mol^{-1}$. For intermediate tetragonal spinels, the enthalpy of transition to cubic appears to diminish strongly with increasing iron content but has not been quantified.

Acknowledgments

References

[1] B. Mason, Geol. Fören. Föreh. Stockholm Föerh. 65 (1943) 97.
[2] H.F. Mc Murdie, B.M. Sullivan, F.A. Maur, Natl. Bur. Standards Res. 45 (1950) 35.
[3] H.J. Van Hook, M.L. Keith, Am. Miner. 43 (1958) 69.
[4] A. Muan, S. Somiya, Am. J. Sci. 260 (1962) 230.
[5] D.G. Wickham, J. Inorg. Nucl. Chem. 31 (1969) 313.
[6] B. Von Punge-Witteler, Z. Phys. Chem. 143 (1984) 239.
[7] T. Tsuji, Y. Asakura, T. Yamashita, K. Naito, J. Solid State Chem. 50 (1991) 273.
[8] L. B. Pankratz, US Bureau of Mines Bulletin 672, 1982.
[9] L. Cervinka, R. Hosemann, W. Vogel, Acta Crystallogr. A 26 (1969) 277.
[10] P. Holba, M.A. Khilla, S. Kupricka, J. Phys. Chem. Solids 34 (1973) 387.
[11] S. Guillemet-Fritsch, S. Viguié, A. Rousset, J. Solid State Chem. 146 (1999) 245.
[12] Yu.D. Tret'yakov, Inorg. Mater. 1 (3) (1965) 374.
[13] V.I. Roshchupkin, V.I. Lavrent'ev, Inorg. Mater. 2 (4) (1966) 612.
[14] V.I. Roshchupkin, V.I. Lavrent'ev, Inorg. Mater. 3 (3) (1967) 490.
[15] T.I. Bulgakova, A.G. Rozanov, Russ. J. Phys. Chem. 44 (7) (1970) 910.
[16] L.A. Reznitskii, Inorg. Mater. 10 (3) (1974) 408.
[17] A. Navrotsky, I. Inorg. Nucl. Chem. 31 (1969) 59.
[18] Yu.D. Tret'yakov, Z. Neorg. Khim. 9 (1964) 161.
[19] K. Schwerdtfeger, A. Muan, Trans. Met. Soc. AIME 239 (1967) 1114.
[20] A. Muan, S. Somiya, Am. J. Sci. 269 (1962) 230.
[21] L.A. Reznitskii, K.G. Khomyakov, Vestnik Moskov. Univ. Ser. 2: Khimiya 15 (1960) 24.
[22] S. Fritsch, A. Navrotsky, J. Am. Ceram. Soc. 79 (7) (1996) 1761.
[23] S. Fritsch, J.E. Post, S.L. Suib, A. Navrotsky, Chem. Mater. 10 (1996) 474.
[24] C. Laberty, A. Navrotsky, Geochim. Cosmochim. Acta 62 (17) (1998) 2905.
[25] J. Majzlan, K.D. Grevel, A. Navrotsky, Am. Miner. 88 (2003) 855.
[26] A. Navrotsky, Phys. Chem. Miner. 2 (1977) 89.
[27] A. Navrotsky, Phys. Chem. Miner. 24 (3) (1997) 222.
[28] F. Tessier, A. Navrotsky, R. Niewa, A. Leineweber, S. Kikkawa, M. Takahashi, F. Kanamaru, F.J. DiSalvo, Solid State Sci. 2 (2000) 457.
[29] J. Cheng, Ph.D. Thesis, University of California at Davis, 2004.
[30] J. Rodriguez-Carjaval, Programme Fullprof, Proceedings of the Satellite Meeting of the XVth Congress of the International Union of Crystallography on Powder Diffraction, Toulouse, 1990, p. 127.
[31] G.I. Finch, A.P.B. Sinha, K.P. Sinha, Proc. Roy. Soc. A 242 (1957) 28–35.
[32] T. Battault, R. Legros, A. Rousset, J. Eur. Ceram. Soc. 15 (1995) 1141.
[33] T. Battault, R. Legros, A. Rousset, J. Mater. Res. 5 (1998) 1238.
[34] Ph. Tailhades, A. Rousset, R. Bendaoud, A.R. Fert, B. Gillot, Mater. Chem. Phys. 17 (1986) 521.
[35] O. Knacke, O. Kubaschewski, K. Hesselmann, Thermochemical Properties of Inorganic Substances, 2nd ed, Springer, Berlin, Germany, 1991.
[36] R.A. Robie, B.S. Hemingway, J.R. Fisher, US Geol. Survey Bull. 1456 (1995) 456.
[37] F.W. Harrison, C.J. Kriessman, S.R. Pollack, Phys. Rev. 110 (4) (1958) 844.
[38] J. Broz, K. Svatopluk, K. Zaveta, Czech. J. Phys. 9 (1959) 481.
[39] V.L. Moruzzi, J. Appl. Phys. 32 (3) (1961) 59S.
[40] R. Gerber, Z. Simsa, M. Vichr, Czech. J. Phys. B 16 (1966) 912.
[41] G.I. Finch, A.P.B. Sinha, K.P. Sinha, Proc. Roy. Soc. A 242 (1957) 28.
[42] A.H. Eschenfelder, J. Appl. Phys. 29 (3) (1958) 378.
[43] S. Krupicka, K. Zaveta, Czech. J. Phys. 9 (1959) 324.
[44] V.A.M. Brabers, P. Dekker, Phys. Stat. Sol. 29 (1968) K73.
[45] L. Cervinka, R. Hosemann, W. Vogel, Acta Crystallogr. A 26 (1970) 277.
[46] J.A. Kulkarni, V.S. Darshane, Thermochim. Acta 93 (1985) 473.
[47] W. Wolski, E. Wolska, J. Kaczmarek, P. Piszora, Phys. Stat. Sol. (a) 152 (1995) K19.
[48] A. Navrotsky, O.J. Kleppa, J. Inorg. Nucl. Chem. 29 (1967) 2701.
[49] H. St. O'Neill, A. Navrotsky, Am. Miner. 68 (1983) 181.